SUPPLEMENTARY MATERIAL

Endocytic Trafficking and Recycling Maintain a Pool of Mobile Surface AMPA Receptors Required for Synaptic Potentiation

Enrica Maria Petrini[1,2], Jiuyi Lu[3], Laurent Cognet[4], Brahim Lounis[4], Michael D. Ehlers[3,5], Daniel Choquet[1]

[1]Laboratoire Physiologie Cellulaire de la Synapse, University of Bordeaux and CNRS, 33077 Bordeaux, France.

[2]Department of Neuroscience and Brain Technology, Italian Institute of Technology, Genoa, Italy

[3]Department of Neurobiology, Duke University Medical Center, Durham, North Carolina 27710, USA

[4]Centre de Physique Moléculaire Optique et Hertzienne, University of Bordeaux and CNRS, 33405 Talence, France,

[5]Howard Hughes Medical Institute, Duke University Medical Center, Durham, North Carolina 27710, USA

SUPPLEMENTARY DATA

Identification of synapses and EZs

To investigate the lateral mobility of surface AMPARs at synapses and EZs, we took advantage of the site-specific accumulation of Homer and Clathrin at PSDs and clathrin rich zones, respectively (Ehrlich et al., 2004; Foa et al., 2001; Brakeman et al., 1997). We imaged Homer::GFP and Clathrin::DsRed expressed in cultured hippocampal neurons by dual channel live cell fluorescence. Homer::GFP was reliably juxtaposed to the pre-synaptic marker v-Glut (Figure S1A). Virtually all Homer::GFP-containing synapses contained endogenous PSD-95 immunoreactivity (99 ± 1 %) and exhibited a density along dendrites comparable to non-transfected sister cells (Figure S1B). Similar results were obtained when Homer::GFP and Clathrin::DsRed were cotransfected (Figure S1E). Furthermore, Homer and Clathrin overexpression did not affect either synaptic activity (Figure S1C-D) or the intensity of synaptic GluR1 clusters compared to untransfected neurons (Figure S1F). It has been previously demonstrated that Clathrin::DsRed colocalizes and shares the same dynamics with σ2-AP2 thus leaving CCPs assembly unaffected (Ehrlich et al., 2004). Altogether Homer::GFP and Clathrin::DsRed proved to be reliable reporters for respectively localizing synapses and clathrin-rich zones, without detectable structural or functional effects on synapses.

GluR1-QD complexes can be internalized through clathrin-mediated endocytosis

As a control, we studied receptor internalization in control conditions and upon blockade of clathrin-mediated endocytosis by the expression of GTPase-deficient Dyn2-K44A::EGFP (Figure S2A). Confocal microscopy in live neurons revealed that in control neurons GluR1-QD

complexes could be internalized over 30 minutes, while in Dyn2-K44A neurons GluR1-QD complexes were almost exclusively at the surface at the end of the same period (Figure S2B) thus unequivocally proving that GluR1-QD complexes can be internalized through a clathrin-mediated process..

In order to verify that in our experiments we were indeed imaging surface GluR1-QD complexes we used the acid strip to remove surface antibodies (Figure S2C). Confocal microscopy of live QD-decorated neurons revealed exclusively intracellular (soma and dendrites) QDs when time for endocytosis was allowed. In contrast only surface QD were detected when the acid strip was performed right after QD-labelling (Figure S2D). Due to the difficulty in distinguishing surface from endocytosed receptors during real time fluorescence imaging, we limited single particle tracking to 10 min after QD staining, a time period during which very modest endocytosis occurs in the absence of stimulation (Figure S2C-D) (Tardin et al., 2003; Lin et al., 2000).

The dynamics of AMPARs at synapses is influenced by the Synapse to EZ distance

At most synapses, PSD and EZ were adjacent. A small percentage of PSDs lacked nearby endocytic zones (20%) and a few PSDs overlapped with EZs (~10%) since they were too close to be optically resolved. In those latter cases, AMPARs dynamics was more similar to that in compartments exclusively labelled by Clathrin::DsRed than by Homer::GFP (Figure S3A-B). This suggests that within synaptic domains, AMPARs on the overlap region might belong to EZ. In the light of this evidence and the low occurrence of EZ/syn overlap, overlying synapses and EZs were removed from further analysis.

We then directly investigated the influence of synapse-EZ proximity on receptor dynamics. To this end, the diffusion coefficient of each mobile synaptic receptor was measured

as a function of the distance separating the controid of the synapse where it was located from that of the nearest clathrin spot (Figure S3C). GluR1 receptors moved faster inside synapses close to EZs, compared to those remote from EZs, as shown by the inverse correlation between receptor diffusion coefficients and syn-clathrin distances (Figure S3C, left panel). In contrast, receptor diffusion on clathrin was independent of the distance from the nearest synapse, suggesting that GluR1 dynamic behaviour is comparable at EZ and CCPs (Figure S3C, right panel). Altogether, those data suggest a specific influence of the proximity of EZs on receptor lateral mobility inside synapses (Figure S3D and Suppl. Movie 3).

GluR1 mobility in Dyn3-PL expressing neurons is not influenced by the Synapse to clathrin distance

In Dyn3-PL neurons there was no correlation between the diffusion coefficient of synaptic receptors at a given synapse and the distance from the closest EZ (Figure S4A). Interestingly, receptor diffusion coefficients at Dyn3-PL synapses were comparable to those in endogenous EZ-negative synapses of Dyn3-Wt neurons (Figure S4A and S3C). In contrast, receptor mobility on clathrin puncta was comparable in untransfected and Dyn3-Wt or Dyn3-PL transfected neurons, and independent of the distance from a nearby synapse (Figure S4B-E). This indicates that the transient stabilization of AMPARs at clathrin-rich zones is not influenced by the vicinity of synapses.

Endogenous Dyn3 is required for sustaining the presence of a mobile pool of AMPARs at synapses

As an alternative way to investigate the effect of Dyn3 disruption, we employed RNA interference (RNAi) to knock down endogenous Dyn3 (Lu et al., 2007). Neurons were

transfected with Homer::DsRed to identify synapses along with either the short hairpin RNA (shRNA) d3RNAi-2 that recognizes Dyn3 or a scrambled shRNA control. Similar to Dyn3-PL, the expression of d3RNAi-2 induced a loss of EZ-positive synapses (Lu et al., 2007) and depleted synapses of mobile GluR1-containing AMPARs. This was illustrated by a stronger confinement (Figure S5A), an increased fraction of immobile receptors at synapses, a decreased diffusion of mobile receptors and an increased dwell time of exchanging receptors at synapses (Figure S5B). Altogether these data indicate that endogenous Dyn3 is required for maintaining a mobile pool of receptors at synapses.

Impairment of AMPARs interaction with the endocytic machinery reduces receptor trapping at EZs and depletes synapses of mobile receptors

In order to test the dependence of GluR1 transient trapping at EZs on its interaction with the endocytic machinery, we used the GluR1-R838A mutant unable to bind AP2 (Lee et al., 2002). We first verified that overexpressed GluR1-R838A was less endocytosed than GluR1-Wt with a live cell antibody feeding (Figure S7A-B). We then measured the mobility of GluR1-R838A at EZs. The transient trapping of GluR1-R838A at clathrin-rich zones was significantly lower than that observed for GluR1-Wt. Similarly, at clathrin puncta both the percentage of immobile GluR1-R838A and the dwell time of exchanging receptors was significantly reduced relative to GluR1-Wt (% immobile: R1-Wt = 50±3%, n= 415; R1-R838A = 42±2%, n= 359; $p<0.05$. Mann-Whitney U test; dwell times: GluR1-Wt, 1.54 ± 0.08 s; GluR1-R838A, 1.31 ± 0.06 s, $p<0.05$, Mann-Whitney U test, not shown). Therefore we conclude that receptor trapping at EZs depends on receptor interaction with AP-2 adaptor proteins.

The impaired interaction of GluR1-R838A with the endocytic machinery reduces AMPARs internalization (Lee et al., 2002), thus decreases receptor recycling. Given that reduced

recycling induced by Dyn3-PL overexpression decreases synaptic receptor accumulation and mobility, we examined the abundance and surface dynamics of GluR1-R838A at synapses. Immunocytochemical approach revealed a significant reduction in GluR1-R838A accumulation at synapses compared to GluR1-Wt (Figure S7C). These less numerous receptors exhibited reduced mobility at synapses as evidenced by a more curved MSD versus time function (Figure S7D). Accordingly, mobile synaptic GluR1-R838A exhibited a smaller diffusion coefficient and a longer dwell time compared to GluR1-Wt (Figure S7E). Thus, both the physical proximity of the EZ and interaction with clathrin adaptors is required to maintain a mobile pool of AMPARs at synapses.

Uncoupling EZ from PSD renders synapses insensitive to Glycine-induced potentiation

In order to refine the study of Gly potentiation of excitatory synaptic transmission, a time course analysis was performed by pooling mEPSCs events into 10 min epochs (Figure 5E). In Dyn3-Wt expressing neurons, a significant increase of mEPSCs amplitude was found 10 min after Gly stimulation. This potentiation declined over time and reached control values at 40 min. In contrast, in Dyn3-PL neurons, Gly stimulation failed to significantly increase mEPSC amplitudes, although the values were constantly larger than in control conditions. Even though these experiments monitor synaptic strength across the entire population of inputs, it is appropriate to conclude that EZs displacement causes a global lack of synaptic potentiation.

SUPPLEMENTARY DISCUSSION

Are the effects of mutant Dyn3 only due to impaired receptor recycling?

We show that a mutant Dyn3, previously demonstrated to displace EZs from the PSD vicinity and to impair receptor recycling (Lu et al., 2007), depletes the mobile pool of synaptic receptors. Previous studies have shown that Dyn3 associates with the actin-interacting protein cortactin (Gray et al., 2005; Cao et al., 2003), thus revealing an indirect link between dynamin and the intracellular machinery for actin assembly (Schafer, 2004). Therefore, impairment of Dyn3 could indirectly interfere with actin dynamics (Zhu et al., 2005) and cell shape. The lack of differences in the FRAP of F-actin in neurons expressing Wt and mutants of Dyn3 argues against this possibility (Lu et al., 2007). Moreover unaltered PSD-95 density and intensity at synapses upon EZs displacement rules out an indirect effect through perturbation of scaffold proteins.

Although Dyn3 impairment was cell wide, receptor lateral mobility was exclusively affected at synapses. This strongly argues against the possibility of a cell wide indirect effect on receptor dynamics. The unchanged total surface GluR1 expression between Dyn3 and Dyn3-PL transfected neurons and the unaffected levels of total AMPARs observed upon inhibition of endocytic recycling (Park et al., 2004) rules out the alternative interpretation that reduced synaptic receptors might be a result of diminished total receptor expression. Therefore we favour the interpretation that depletion of mobile receptors at synapses (by uncoupling EZs from the PSD, by interfering with receptor-AP2 interaction and by impairing endosomal recycling) is a direct consequence of impaired receptor recycling.

Synaptic potentiation and mobile AMPARs

Activity-dependent regulation of AMPAR number at synapses is one of the major postsynaptic effectors of synaptic plasticity (Shepherd and Huganir, 2007; Malenka and Bear, 2004). Although it is not possible to induce LTP in cultured neurons, several reports have proved the possibility to chemically promote a lasting increase in synaptic transmission though the activation of NMDA receptors with Gly (Lau and Zukin, 2007; Serulle et al., 2007; Lu et al., 2001). Notably, Gly-induced potentiation, reflecting tetanus-induced LTP (Shi et al., 1999), was associated with increased AMPAR abundance at synapses due to promoted exocytosis (Kopec et al., 2006; Park et al., 2004; Liao et al., 2001; Lu et al., 2001; Passafaro et al., 2001), as confirmed by our data. The lack of effect of anisomycin, a potent blocker of protein synthesis, on Gly-induced exocytosis (Park et al., 2004), rules out the contribution of *de novo* receptor synthesis and supports the importance of receptor recycling on synaptic potentiation. Our results show that when EZ are close to PSD, Gly-induced potentiation of mEPSCs amplitude and increase in synaptic receptor accumulation are associated with a global immobilization of synaptic AMPARs. These results are consistent with the slower kinetics and larger immobile fraction of GluR1 previously observed with FRAP after Gly stimulation (cLTP) in the time span of our experiments (Sharma et al., 2006).

SUPPLEMENTARY METHODS

Plasmid Constructs

DsRed fusion of the Clathrin Light Chain (LCa) was kindly provided by Dr. Kirchhausen. EGFP and DsRed -tagged Homer 1C were generated subcloning Homer 1C cDNA into the eukaryotic expression vector pcDNA3 (Invitrogen) at the EcoRI site and then either EGFP or DsRed were inserted at the N-terminus of the Homer 1C sequence between the Hind III/EcoRI sites. Enhanced GFP and mCherry were expressed from the pEGFP-N1 and pmCherry-N1 vectors, respectively (Clontech). Dyn3, Dyn3-PL constructs were previously described (Lu et al., 2007). Rab11a Wt and Rab11a S25N were generated by subcloning the Rab11a Wt and the mutated Rab11a-S25N DNA sequences from GFP containing constructs, into a pcDNA vector (Invitrogen). GluR1-R838A was obtained by introducing an Arginine to Alanine point mutation in position 838 of the Wt sequence of GluR1 according to Lee 2002, with the Quickchange mutagenesis Kit (Stratagene, France). All constructs were verified by DNA sequencing.

Primary neuronal cultures and transfection

Cultures of hippocampal neurons were prepared from E18 Sprague-Dawley rats following a previously described method (Goslin, 1998). Cells were plated at a density of 100 - 200 x 10^3 cells/ml on polylysine pre-coated coverslips and kept in serum free neurobasal medium (Invitrogen) at 37°C in 7.4 % CO2 for 16-18 days in vitro (DIV). During this period half of the medium was exchanged weekly.

Neurons were transfected at 5 DIV using Effectene (Qiagen) following the company protocol.

Antibodies and drugs

The antibody against the N-terminal epitope of the GluR1-subunit was kindly provided by R. Huganir (Mammen et al., 1997). Fluorescent secondary antibodies (Alexa 568 and 647) against rabbit IgG as well as goat F(ab')2 anti-Rabbit IgG Conjugate (H+L) highly cross-adsorbed QD655 were from Invitrogen (France). TTX, Picrotoxin, APV from Tocris (UK), Glycine, Strychnine and all other chemicals mentioned were purchased from Sigma/Aldrich (France). Unless otherwise stated drugs were bath applied. In the case of Gly application during QD imaging and the corresponding control, the solution was delivered through a puffer pipette positioned close to the ROI in order to reduce diffusion limited delays in medium exchange.

Acid strip

An acid strip protocol consisted of 1 minute incubation in the culture medium at pH = 2.4, 10°C of live neurons previously labelled either with only anti GluR1 antibody or consecutively with anti GluR1 antibody and QDs. In the first case the presence of surface receptor-bound antibodies was detected in fixed unpermeabilized neurons with a secondary antibody imaged on an epifluorescence microscope. In the second case QD-coupled antibodies were imaged in live neurons with confocal microscopy. In both cases the acid strip was compared to a control treatment consisting of incubation in cold culture medium (pH = 7.4, 10°C for 1 minute). In order to promote receptor endocytosis, 30 minutes incubation of QD-labelled neurons at 37°C was allowed.

QD labelling and live cell imaging

QD staining of surface AMPARs was performed as previously described (Bats et al., 2007). Briefly, neurons were incubated with anti-GluR1 antibody (0.5 mg/ml) for 10 minutes at room

temperature (rather than at 37°C, in order to limit receptor endocytosis) and then were incubated with QDs at a final concentration of 0.1 nM for 2 minutes at room temperature.

For QD imaging, 1200 consecutive frames were acquired at 20 Hz with a EM-CCD camera (Cascade II, Roper Scientific) using Metamorph software (7.0, Universal Imaging Corp.). For EGFP and DsRed, images were obtained with an integration time of 50–100 ms. Samples were illuminated with a mercury lamp (Olympus, France). EGFP, DsRed and QD fluorescence signals were detected with appropriate excitation (HQ480/20, HQ525/50 and HQ 565/30, respectively, Chroma Technology Corp.) and emission filters (HQ 525/40, HQ 605/20 and 655WB20, respectively) dually controlled by filter wheels. While fluorescence spectra of EGFP and DsRed are far enough to be resolved, that of QD655 partially overlaps the tail of DsRed emission. The bandwith of the emission filter for DsRed excludes QD655 fluorescence, but it is possible that DsRed contaminates QD655 signal. However the large morphological and intensity differences found in single particle and bulk DsRed signals allowed unequivocally selecting QD655 fluorescence in image processing for the Single Particle tracking (see appropriate paragraph). Live cells were imaged at 37°C in an open chamber filled with the same solution used for electrophysiological recordings (see below), mounted onto an inverted microscope (IX71, Olympus, France) equipped with a 100X oil-immersion objective (NA = 1.4).

Using the 100X objective, the camera pixel size was 160nm. According to the estimations for synapse and clathrin-rich zones diameters (200-500 nm and 100-200 nm, respectively) (Chen et al., 2005; Ehrlich et al., 2004), the size of both compartments is comparable or slightly larger than the diffraction limit, thus providing apparent fluorescent spots with typical diameters of 2-4 and 1-2 pixels, respectively. Although the definition of the compartments was diffraction limited, the sub-wavelenght pointing accuracy of the single particle detection allowed accurate description of receptor mobility within such small regions. The dwell time of QDs was measured

from trajectories duration of exchanging QD that were not present at the region at the end of the experiment. This exclusion minimizes a biased calculation of the dwell time that otherwise would reflect the duration of the acquisition epoch for long-dwelling particles.

Continuous tracking of single QDs was performed between blinks with custom software written within MATLAB (The Mathworks Inc., Natick, MA). The method is based on a QD maximal allowable displacement (4 pixels) during a maximal allowable duration of the dark period (25 frames, corresponding to 1.25 s acquisition). Instantaneous diffusion coefficients, D, were calculated as previously described (Tardin et al., 2003) from linear fits of the n = 1 to 8 values of the mean squared displacement (MSD) *versus* time plot, according to the equation: MDS(t) = <r2> = 4Dt for 2D-diffusion. MSD(t) was calculated according to the formula:

$$\langle r2 \rangle = [_{i=1}\Sigma^{(N-n)}(X_{i+n} - Xi)^2 +)(Y_{i+n} - Yi)^2 /N - n]dt$$

for reconstructed trajectories of more than 100 frames.

Direct measure of receptor exocytosis

Surface SEP-GluR1 was first bleached in a large portion of dendrites ("large bleach") and fluorescence recovery was monitored in the bleached region over 20 minutes (Figure S8A). Return of fluorescence by lateral diffusion in bleached dendrites was blocked by continuously bleaching a small barrier at the edge of the bleached region where surface fluorescent receptors would imperatively pass to laterally diffuse from non-bleached regions. Implementation of this protocol allowed isolating fluorescence recovery due to receptor exocytosis from that due to surface diffusion (Figure S8B). Receptor exocytosis was normalized to pre-bleach values (Figure 4B). For quantification of receptor exocytosis SEP fluorescence detected 20 minutes after "large bleach" was normalized to that measured at the beginning of the experiment, setting to zero the

residual fluorescence signal right after bleach. Overexpression of Homer::DsRed allowed identification of synapses (Figure 4A).

Confocal Imaging

Confocal imaging was performed at the PICIN imaging center of the Neurosciences Institute of the University of Bordeaux II using a Leica TCS SP2 laser scanning confocal microscope with excitation lines from a 458 nm, 488nm and 543 nm lasers (SpectraPhysics) in the sequential mode. QD-specific fluorescence signal was confirmed by spectral analysis. Images were acquired using an oil immersion 63 X (NA 1.32) Plan Apochromat objective and analyzed using Imaris (Bitplane).

Electrophysiology

Miniature excitatory postsynaptic currents (mEPSCs) were recorded in the whole-cell configuration of the patchclamp technique. Patch electrodes, formed from thin borosilicate glass (Hilgenberg, Malsfeld, Germany) had a resistance of 3-5 MΩ when filled with an intracellular solution containing (in mm) CsCl, 137; CaCl2, 1; MgCl2, 2; 1,2-bis(2-aminophenoxy)ethane-N,N,N',N'-tetraacetic acid (BAPTA), 11; ATP, 2; and HEPES, 10; pH 7.2 with CsOH. The composition of the external solution (also used for imaging) was (in mm) NaCl, 137; KCl, 5; $CaCl_2$, 2; $MgCl_2$, 1; glucose, 20 and HEPES, 10; pH 7.4. In the Gly stimulation protocol $MgCl_2$ was replaced with NaCl. mEPSCs were recorded at 37°C from a holding potential of -60 mV in the presence of tetrodotoxin (TTX; 1mM), 2-amino-5-phosphonovalerate (APV, 50 μM) and picrotoxin (100μM). The stability of the patch was checked by repetitively monitoring the input and series resistance during the experiments. Cells exhibiting 10–15% changes were excluded

from the analysis. Currents were sampled at 20 kHz and digitally filtered at 3 kHz with Pulse-Pulse fit software version 8.62, using a EPC 10 double patch-clamp amplifier (both from HEKA Electronics, Lambrecht, Germany). mEPSC were analysed with Clampfit 9.0 using an algorithm based on a sliding template. The threshold for detection was set at 3.5 times the SD of the baseline noise.

Statistics

Statistical values are given as mean ± S.E.M. or medians ± interquartile range (IQR) defined as the interval between 25% - 75% percentile. Statistical significances were tested using Prism 4.0 (GraphPad, USA). Normally distributed datasets were compared using the unpaired Student's t-test. Statistical significance between more than two normally distributed datasets was tested by one way ANOVA variance test followed by a Newman-Keuls test to compare individual pairs of data. Non-Gaussian data sets were tested by non-parametric Mann-Whitney test. Indications of significance correspond to p-values < 0.05 (*), $p < 0.01$ (**) and $p < 0.001$ (***). For QD tracking, for each experiment indicated is the number of trajectories reconstructed from at least 53 different fields observed in at least 15 different trials. For immunocytochemistry n represents the number of neurons observed. For the FRAP experiments, n indicates the number of synaptic or extrasynaptic regions imaged.

Immunocytochemistry

Live staining of native GluR1 subunit-containing receptors was performed by incubating the neurons with the same anti GluR1 antibody used for QD labelling at 0.5 mg/ml in the culture medium at room temperature for 10 minutes. In the experiments focusing on synaptic

potentiation, the antibody was applied 10 minutes after Glycine stimulation. After fixation with paraformaldeide 4% supplemented with sucrose 4% for 10 minutes, neurons were incubated with Alexa 647-conjugated secondary antibody (Invitrogen, France) for 1 hr at room temperature. Control experiments without the primary antibody were performed to test fluorescent signal arising from aspecific binding of the seconday antibody. Coverslips, mounted in Mowiol mounting medium, were obserbed with a wide-field upright epifluorescence microscope (DM R, Leica) using a CCD camera (Coolsnap HQ, Photometrics). Fluorescnce signals from acquired images were analysed using Metamorph (7.0, Universal Imaging Corp.).

SUPPLEMENTARY FIGURE LEGENDS

Figure S1. Recombinant Homer and Clathrin are reliable reporters for synapses and clathrin-rich zones

(A) Homer1::EGFP is expressed juxtaposed to the presynaptic protein VGlut (left). On the right a higher magnification of the insets on the left. Scalebars 10 and 1 μm. (B) Homer1 is a reliable marker of endogenous synapses. Neurons transfected with EGFP::Homer (top, left) were immunolabelled with anti-PSD-95 antibody (top, right). The merge of two signals indicates that Homer and PSD-95 colocalize (bottom, left). Scalebar 10 μm. Bottom right: quantification of synapse density. Data (mean ± SEM) are expressed as PSD-95 clusters/μm in untransfected neurons and Homer::EGFP transfected sister cells. (n=20 in each condition, $p>0.05$, Student's t test). (C) Homer::EGFP and Clathrin::DsRed overexpression does not affect synaptic transmission. Example traces of mEPSCs (left) recorded from untransfected (a) and transfected (b) sister cells indicated in the middle (transmitted light) and right panel (fluorescence of overexpressed Homer::EGFP and Clatrhin::DsRed). Scalebar 10 μm, (D) Quantification of the amplitude (left) and frequency (right) of mEPSCs recorded from untransfected and transfected neurons. n=7 and 7, $p>0.05$ (ns), Student's t test. (E) Overexpression of Homer, Clathrin and Dyn3 does not affect synapse density. Homer clusters/μm in neurons transfected with: Homer = 27.3 ± 2.4; Homer+Clathrin= 27.2 ± 2.4; Homer+Clathrin+Dyn3= 27.7 ± 4.2. Data are expressed as the mean (±SEM). n=20 in each condition, $p>0.05$, One way ANOVA. (F) Synaptic accumulation of GluR1 is not affected by the presence of recombinant Homer, Clathrin and Dyn3. Average synaptic GluR1 fluorescence intensity/pixel (a.u.): untransfected = 111.7±5.8; Homer+Clathrin = 105.0±9.9; Homer+Clathrin+Dyn3 = 104.1±7.9, n=20 in each condition, one way ANOVA.

Figure S2. GluR1-QD complexes can be internalized through clathrin-mediated endocytosis

(A) The Dyn2-K44A mutant impairs clathrin-mediated endocytosis. Internalized TfR in neurons transfected with either mCherry alone (ctrl) or along with Dyn2-K44A::GFP. Note the comparable TfR abundance in the untransfected cells reported in both cases. Scalebar 10 μm. (B) GluR1-QD complexes are endocytosed with a clathrin-mediated process. XZ confocal sections (2μm thick) of neurons expressing mCherry alone (ctrl) or with Dyn2-K44A, labelled with antiGluR1-QDs. Note the reduced number of internalized QDs in Dyn2-K44A neurons. Scalebar 10 μm. (C) Acid strip of surface antibodies. Left, example pictures of surface GluR1 receptors in neurons exposed either to a control cold solution (top) or to the acid strip (bottom). Right, corresponding transmitted light images of the neurons on the left. Scalebar 10 μm. (D) Without promoting endocytosis, GluR1-QD complexes are mainly at the surface. XZ confocal sections (2 μm thick) of confocal stacks of GluR1-QD complexes (red) imaged in live neurons expressing soluble EGFP (green) as a cell fill. Surface complexes (red) and intracellular ones (yellow) can be distinguished. Neurons exposed to a control treatment (top) or to the acid strip (bottom) with or without appropriate incubation to allow endocytosis are reported. Scalebar 10 μm.

Figure S3. The presence of EZ close to the PSD affects AMPAR mobility only at synapses

(A-B) GluR1 mobility at partially overlapping synapses and EZs. (A) Classification of "tot", "pure" and "overlap" regions of partially overlapping (yellow) EZ (red) and synapse (green). The trajectory of a single QD exploring the "EZ pure" (red), the "overlap" (yellow) and the "syn pure" (green) regions is shown. Extra-EZ-extra-syn regions (black) are only partially represented. (B) MSD *versus* time plot of GluR1-QD complexes found at "syn pure" and "overlap" regions (left)

or "EZ pure" and "overlap" zones (right). (C) Left: GluR1 is more mobile at synapses exhibiting an adjacent EZ. Diffusion coefficients of GluR1-QD complexes at synapses (left or clathrin, right) plotted as a function of the distance from the closest clathrin puncta (or synapse, right). (D) Diffusion coefficient *versus* time plot of a QD-receptor complex exploring a synapse (#1) adjacent to an EZ (red) and than an isolated synapse (#2). The corresponding trajectory of the particle is reported in the inset with the same color code. Note the higher mobility of the particle in synapses #1.

Figure S4. Dyn3-PL selectively reduces synaptic GluR1 diffusion at synapses

(A) Diffusion coefficients of mobile GluR1-QD complexes at synapses as function of the distance from the synapse explored by the QD to the closest clathrin puncta in Dyn3 Wt (full circles, see Figure S3) and in Dyn3-PL neurons (empty circles). Note that data points from Dyn3 at larger distances (endogenous EZ-negative synapses) are comparable to data points referring to Dyn3-PL (recombinant EZ-negative synapses). (B) The same type of plot as in (A), referred to QDs at clath and to the distance from the explored clathrin spot to the closest synapses. (C-E) Uncoupling EZ from the PSD does not influence GluR1 mobility at EZs. (C) MSD versus time plot of receptor-QD complexes, (D) median diffusion coefficient (± IQR, Mann-Whitney test) of mobile receptors and (E) immobile receptor fraction at clath in Dyn3 (red), Dyn3-PL expressing neurons (dashed red) and in neurons lacking any recombinant form of Dyn3 (empty). Unless otherwise stated data are expressed as mean ± SEM (Student's t test). (F-G) The lateral mobility of receptor-QD complexes at regions simultaneously excluding synapses and clath ("extra") is not affected by the displacement of EZs from the PSD. Quantification of the median diffusion coefficient (± IQR) of mobile receptors (F) and immobile receptor fraction (± SEM) (G) in Dyn3

(black), Dyn3- PL expressing neurons (dashed) and in neurons lacking any recombinant form of Dyn3 (empty).

Figure S5. Endogenous Dynamin-3 is required to maintain mobile AMPA receptors at synapses

(A) Expression of dynamin-3 shRNA (d3RNAi-2) reduces the lateral mobility of GluR1 at synapses. Mean Square Displacement of synaptic GluR1-QD complexes in neurons expressing either d3RNAi-2 or a scrambled shRNA control (scramble). (B) Quantification of immobile fraction (left), median diffusion coefficient (± IQR, Mann-Whitney test) and dwell time of synaptic receptors in neurons expressing either the scramble construct or d3RNAi-2. Unless otherwise stated data are expressed as mean ± SEM and tested with Student's t test. n trajectories =204 and 191, $p<0.05$ (*), $p<0.001$ (***). Note that the surface mobility of synaptic GluR1 receptors was comparable in the presence of scrambled shRNA and in non-transfected neurons (Figure S5A).

Figure S6. Dyn3 overexpression does not alter either GluR1 diffusion at synapses or synaptic structure

(A) Synaptic GluR1 mobility in neurons overexpressing Homer::EGFP and Clathrin::DsRed with or without Dyn3::FLAG or Dyn3-PL::FLAG. The diffusion coefficient (median ± IQR, Mann Whitney test) and the percentage of immobile receptors (mean ± SEM, Student's t test) are reported. Non significant (ns), $p<0.01$ (**), $p<0.001$ (***). (B) The intensity and density of synapses is not affected by the overexpression of any form of Dyn3. Fluorescence intensity/pixel

(left) and density/μm (right) of PSD-95 clusters in neurons transfected as indicated. Data are presented as mean ± SEM, n=20 in each condition, non significant (ns), One way ANOVA.

Figure S7. The interaction of GluR1 to the endocytic machinery is essential for receptor stabilization at EZ and for maintaining mobile AMPARs at synapses

(A) A point mutation of GluR1 in the region interacting with AP2 reduces AMPAR endocytosis. Antibody-based endocytosis assays were performed on hippocampal neurons expressing either GluR1-Wt or GluR1-R838A and internalized GluR1 was visualized at the indicated time points with an antiGluR1 antibody. Scale bar 5μm. (B) Quantification of the results in (A). Data represents mean ± SEM of internalized GluR1 at the indicated time points after incubation at 37ºC, normalized to the total (surface+intracellular). n=20 in each condition. (C) GluR1-R838A is less accumulated at synapses. Quantification of surface expression of GluR1-Wt and GluR1-R838A at synapses (mean fluorescence intensity/pixel ± SEM, n=20-21, $p<0.05$(*), Student's t test). (D) Comparison of GluR1-Wt and GluR1-R838A confinement at synapses. Data represent the average MSD ± SEM at different time points. (E) Reduced mobility of GluR1-R838A-QD complex at synapses. Diffusion coefficient (Mann Whitney test, left), dwell time (middle) and fraction of immobile receptors at synapses. n trajectories = 634 and 554. non significant (ns), $p<0.05$ (*), $p<0.001$ (***), Student's t test unless otherwise stated.

Figure S8. Direct imaging of newly exocytosed AMPA receptors

(A) Example images of a neuron transfected with SEP::GluR1 (a) and Homer::DsRed (to identify synapses, not shown). A large portion of dendritic branches was bleached (dotted region) in order to remove surface SEP fluorescence (b). SEP fluorescence was measured in the bleached region

20 minutes afterwards (c). During this period "optical barriers" (yellow bar) were used to prevent lateral diffusion of non-bleached receptors from neighbouring regions into the bleached one. Different spots in the non-bleached region and in the bleached region with or without barriers are indicated with different colour codes in (c) Scalebar 10 μm. (B) Quantification of SEP::GluR1 fluorescence in the spots indicated in Ac over the protocol. Time points -1 min (a), 0 min (b) and 20 min (c) are indicated consistently with (A). In the absence of optical barriers (violet and orange traces), fluorescence increases over time is due to the combination of exocytosis of new receptors and lateral diffusion of non-bleached receptors from close regions.

Figure S9. Glycine stimulation depletes the recycling pool of AMPARs

(A) Comparison of the protocols used to distinguish Gly-induced exocytosed receptors and Reserve exocytable receptors. The difference consists in performing the "large bleach" before or after Gly stimulation, respectively. (B) Quantification of receptor exocytosis in control conditions (20 minutes after the "large bleach" without stimulation, (red) and during synaptic potentiation. Gly-induced exocyosed receptors (orange) and the reserve exocytable pool (green) are presented. Mean ± SEM. n=74-60 from neurons expressing either Dyn3 or Dyn3-PL.

Figure S10. Local drug application does not affect the surface mobility of receptor-QD complexes

(A) Comparison of the MSD versus time plot of synaptic and extrasynaptic receptor-QD complexes in Dyn3 and Dyn3-PL neurons before and after puffing a control solution close to the recording region for 5 minutes (*i.e.*, at 1 min and 10 min of the experiment, respectively). (B)

Quantification of the diffusion coefficients in the aforementioned conditions. Data are expressed as median ± IQR.

SUPPLEMENTARY MOVIE LEGENDS

Movie S1. AMPARs are slowly mobile at synapses and highly diffusive at extrasynaptic zones.

Recording of the movement of a single QD-bound AMPAR diffusing as a surface of a neurite co-expressing Clathrin-DsRed (red) and Homer-GFP (green). The QD trajectory is yellow and turns blue when the QD blinks. Frames recorded each 50 ms.

Movie S2. AMPARs are slowly mobile at EZ and can diffuse out of EZ.

Recording of the movement of a single QD-bound AMPAR diffusing as a surface of a neurite co-expressing Clathrin-DsRed (red) and Homer-GFP (green). The QD trajectory is initially confined on the endocytic zone and then diffuse out to cross the synapse and exit to the extrasynaptic membrane.

Movie S3. AMPARs are less mobile at EZ- than at EZ+ synapses.

Recording of the movement of a single QD-bound AMPAR diffusing as a surface of a neurite co-expressing Clathrin-DsRed (red) and Homer-GFP (green). The QD trajectory is initially extra-synaptic then displays confined but rapid movement in a synapse bearing an EZ next to it. After alternating between the PSD and the EEZ, it moves to a second EZ-synapse where its movement is much slower.

Movie S4. AMPARs are less mobile at EZ- synapses.

Recording of the movement of a single QD-bound AMPAR diffusing as a surface of a neurite co-expressing Clathrin-DsRed (red) and Homer-GFP (green) in a cell expressing a mutant Dyn3 to

remove EZ from synapses. The QD trajectory is initially extra-synaptic then displays very slow movement at this EZ-synapse.

SUPPLEMENTARY REFERENCES

- Bats, C., Groc, L., and Choquet, D. (2007). The interaction between Stargazin and PSD-95 regulates AMPA receptor surface trafficking. **Neuron** *53*, 719-734.
- Lau, C.G., and Zukin, R.S. (2007). NMDA receptor trafficking in synaptic plasticity and neuropsychiatric disorders. **Nat Rev Neurosci** *8*, 413-426.
- Lu, J., Helton, T.D., Blanpied, T.A., Racz, B., Newpher, T.M., Weinberg, R.J., and Ehlers, M.D. (2007). Postsynaptic positioning of endocytic zones and AMPA receptor cycling by physical coupling of dynamin-3 to Homer. **Neuron** *55*, 874-889.
- Serulle, Y., Zhang, S., Ninan, I., Puzzo, D., McCarthy, M., Khatri, L., Arancio, O., and Ziff, E.B. (2007). A GluR1-cGKII Interaction Regulates AMPA Receptor Trafficking. **Neuron** *56*, 670-688.
- Shepherd, J.D., and Huganir, R.L. (2007). The cell biology of synaptic plasticity: AMPA receptor trafficking. **Annu Rev Cell Dev Biol** *23*, 613-643.
- Kopec, C.D., Li, B., Wei, W., Boehm, J., and Malinow, R. (2006). Glutamate receptor exocytosis and spine enlargement during chemically induced long-term potentiation. **J Neurosci** *26*, 2000-2009.
- Sharma, K., Fong, D.K., and Craig, A.M. (2006). Postsynaptic protein mobility in dendritic spines: long-term regulation by synaptic NMDA receptor activation. **Mol Cell Neurosci** *31*, 702-712.
- Chen, X., Vinade, L., Leapman, R.D., Petersen, J.D., Nakagawa, T., Phillips, T.M., Sheng, M., and Reese, T.S. (2005). Mass of the postsynaptic density and enumeration of three key molecules. **Proc Natl Acad Sci U S A** *102*, 11551-11556.
- Gray, N.W., Kruchten, A.E., Chen, J., and McNiven, M.A. (2005). A dynamin-3 spliced variant modulates the actin/cortactin-dependent morphogenesis of dendritic spines. **J Cell Sci** *118*, 1279-1290.
- Zhu, J., Zhou, K., Hao, J.J., Liu, J., Smith, N., and Zhan, X. (2005). Regulation of cortactin/dynamin interaction by actin polymerization during the fission of clathrin-coated pits. **J Cell Sci** *118*, 807-817.
- Ehrlich, M., Boll, W., Van Oijen, A., Hariharan, R., Chandran, K., Nibert, M.L., and Kirchhausen, T. (2004). Endocytosis by random initiation and stabilization of clathrin-coated pits. **Cell** *118*, 591-605.
- Malenka, R.C., and Bear, M.F. (2004). LTP and LTD: an embarrassment of riches. **Neuron** *44*, 5-21.
- Park, M., Penick, E.C., Edwards, J.G., Kauer, J.A., and Ehlers, M.D. (2004). Recycling endosomes supply AMPA receptors for LTP. **Science** *305*, 1972-1975.
- Schafer, D.A. (2004). Regulating actin dynamics at membranes: a focus on dynamin. **Traffic** *5*, 463-469.

- Cao, H., Orth, J.D., Chen, J., Weller, S.G., Heuser, J.E., and McNiven, M.A. (2003). Cortactin is a component of clathrin-coated pits and participates in receptor-mediated endocytosis. **Mol Cell Biol** *23*, 2162-2170.
- Tardin, C., Cognet, L., Bats, C., Lounis, B., and Choquet, D. (2003). Direct imaging of lateral movements of AMPA receptors inside synapses. **Embo J** *22*, 4656-4665.
- Lee, S.H., Liu, L., Wang, Y.T., and Sheng, M. (2002). Clathrin adaptor AP2 and NSF interact with overlapping sites of GluR2 and play distinct roles in AMPA receptor trafficking and hippocampal LTD. **Neuron** *36*, 661-674.
- Foa, L., Rajan, I., Haas, K., Wu, G.Y., Brakeman, P., Worley, P., and Cline, H. (2001). The scaffold protein, Homer1b/c, regulates axon pathfinding in the central nervous system in vivo. **Nat Neurosci** *4*, 499-506.
- Liao, D., Scannevin, R.H., and Huganir, R. (2001). Activation of silent synapses by rapid activity-dependent synaptic recruitment of AMPA receptors. **J Neurosci** *21*, 6008-6017.
- Lu, W., Man, H., Ju, W., Trimble, W.S., MacDonald, J.F., and Wang, Y.T. (2001). Activation of synaptic NMDA receptors induces membrane insertion of new AMPA receptors and LTP in cultured hippocampal neurons. **Neuron** *29*, 243-254.
- Passafaro, M., Piech, V., and Sheng, M. (2001). Subunit-specific temporal and spatial patterns of AMPA receptor exocytosis in hippocampal neurons. **Nat Neurosci** *4*, 917-926.
- Lin, J.W., Ju, W., Foster, K., Lee, S.H., Ahmadian, G., Wyszynski, M., Wang, Y.T., and Sheng, M. (2000). Distinct molecular mechanisms and divergent endocytotic pathways of AMPA receptor internalization. **Nat Neurosci** *3*, 1282-1290.
- Shi, S.H., Hayashi, Y., Petralia, R.S., Zaman, S.H., Wenthold, R.J., Svoboda, K., and Malinow, R. (1999). Rapid spine delivery and redistribution of AMPA receptors after synaptic NMDA receptor activation. **Science** *284*, 1811-1816.
- Goslin, K.a.B., G (1998). Culturing nerve cells (Cambridge, Massachusetts: MIT Press).
- Brakeman, P.R., Lanahan, A.A., O'Brien, R., Roche, K., Barnes, C.A., Huganir, R.L., and Worley, P.F. (1997). Homer: a protein that selectively binds metabotropic glutamate receptors. **Nature** *386*, 284-288.
- Mammen, A.L., Kameyama, K., Roche, K.W., and Huganir, R.L. (1997). Phosphorylation of the alpha-amino-3-hydroxy-5-methylisoxazole4-propionic acid receptor GluR1 subunit by calcium/calmodulin-dependent kinase II. **J Biol Chem** *272*, 32528-32533.

SUPPLEMENTARY FIGURES:

Figure S1

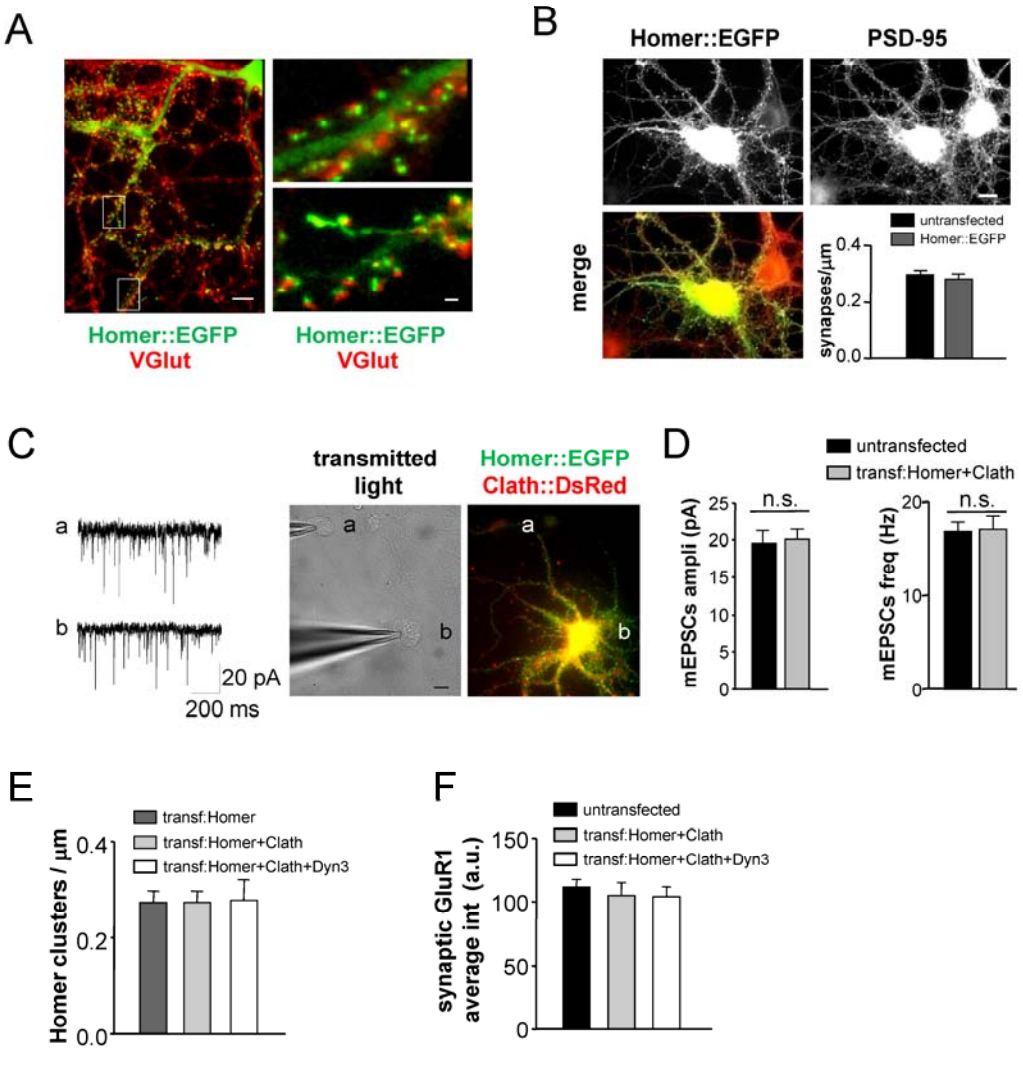
A
Homer::EGFP
VGlut
Homer::EGFP
VGlut
B
Homer::EGFP
PSD-95
merge
untransfected
Homer::EGFP
synapses/µm
0.4
0.2
0.0
C
transmitted light
Homer::EGFP
Clath::DsRed
a
b
20 pA
200 ms
D
untransfected
transf:Homer+Clath
mEPSCs ampli (pA)
n.s.
mEPSCs freq (Hz)
n.s.
E
transf:Homer
transf:Homer+Clath
transf:Homer+Clath+Dyn3
Homer clusters / µm
F
untransfected
transf:Homer+Clath
transf:Homer+Clath+Dyn3
synaptic GluR1 average int (a.u.)

Figure S2

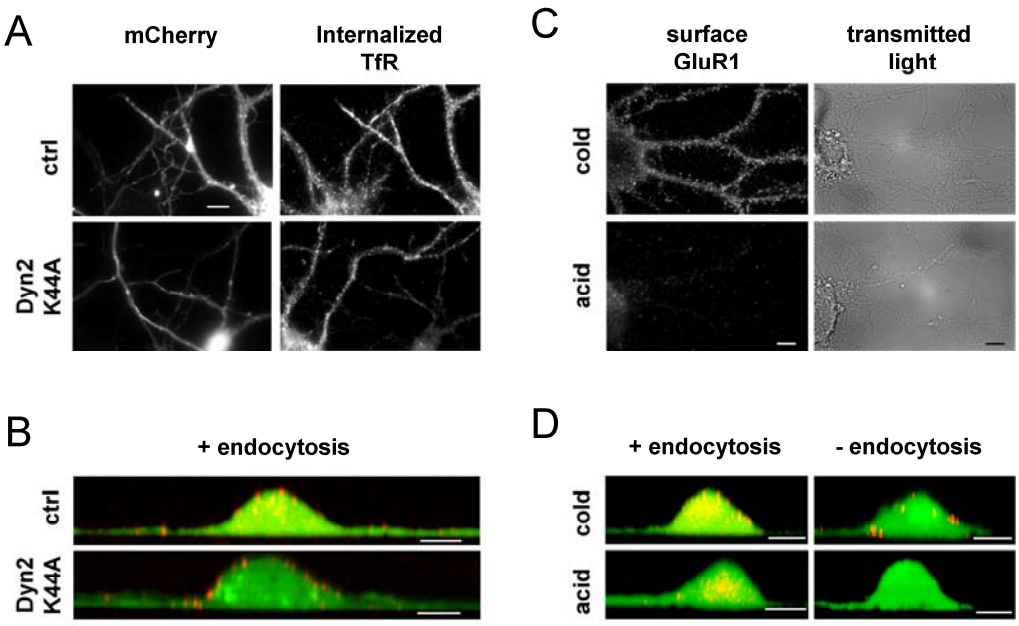
A
mCherry
Internalized TfR
ctrl
Dyn2 K44A
B
+ endocytosis
ctrl
Dyn2 K44A
C
surface GluR1
transmitted light
cold
acid
D
+ endocytosis
- endocytosis
cold
acid

Figure S3

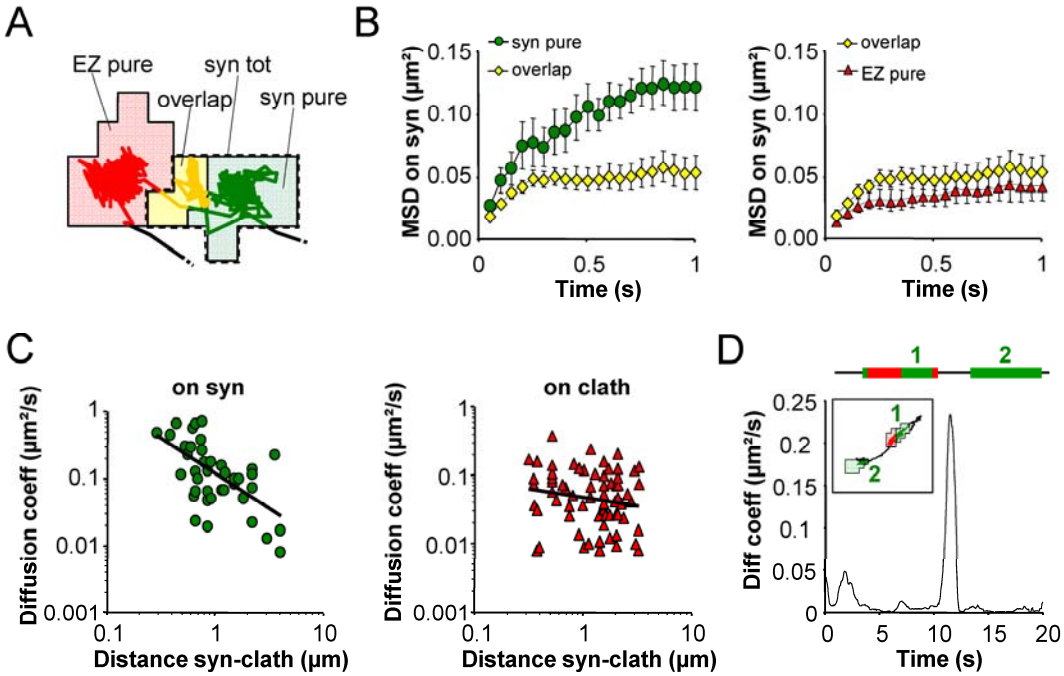
A
EZ pure
syn tot
overlap
syn pure
B
syn pure
overlap
MSD on syn (µm²)
0.15
0.10
0.05
0.00
0
0.5
1
Time (s)
overlap
EZ pure
MSD on syn (µm²)
0.15
0.10
0.05
0.00
0
0.5
1
Time (s)
C
on syn
Diffusion coeff (µm²/s)
1
0.1
0.01
0.001
0.1
1
10
Distance syn-clath (µm)
on clath
Diffusion coeff (µm²/s)
1
0.1
0.01
0.001
0.1
1
10
Distance syn-clath (µm)
D
1
2
Diff coeff (µm²/s)
0.25
0.2
0.15
0.1
0.05
0
0
5
10
15
20
Time (s)

Figure S4

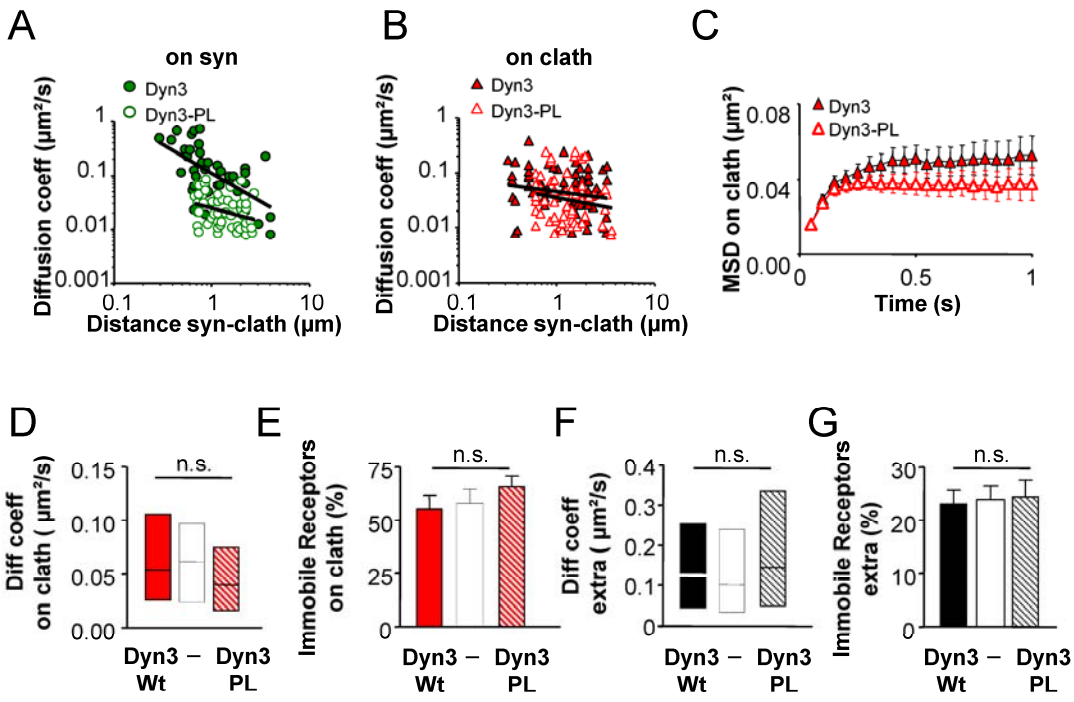
A
on syn
Dyn3
Dyn3-PL
Diffusion coeff (µm²/s)
Distance syn-clath (µm)
B
on clath
Dyn3
Dyn3-PL
Diffusion coeff (µm²/s)
Distance syn-clath (µm)
C
Dyn3
Dyn3-PL
MSD on clath (µm²)
Time (s)
D
Diff coeff on clath (µm²/s)
n.s.
Dyn3 Wt
Dyn3 PL
E
Immobile Receptors on clath (%)
n.s.
Dyn3 Wt
Dyn3 PL
F
Diff coeff extra (µm²/s)
n.s.
Dyn3 Wt
Dyn3 PL
G
Immobile Receptors extra (%)
n.s.
Dyn3 Wt
Dyn3 PL

Figure S5

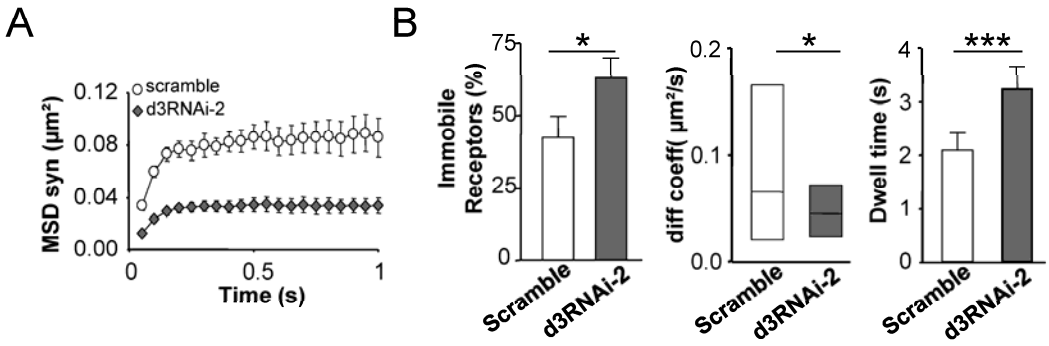
A
B
scramble
d3RNAi-2
MSD syn (µm²)
0.12
0.08
0.04
0.00
0
0.5
1
Time (s)
Immobile Receptors (%)
75
50
25
0
*
Scramble
d3RNAi-2
diff coeff(µm²/s)
0.2
0.1
0.0
*
Scramble
d3RNAi-2
Dwell time (s)
4
3
2
1
0
***
Scramble
d3RNAi-2

Figure S6

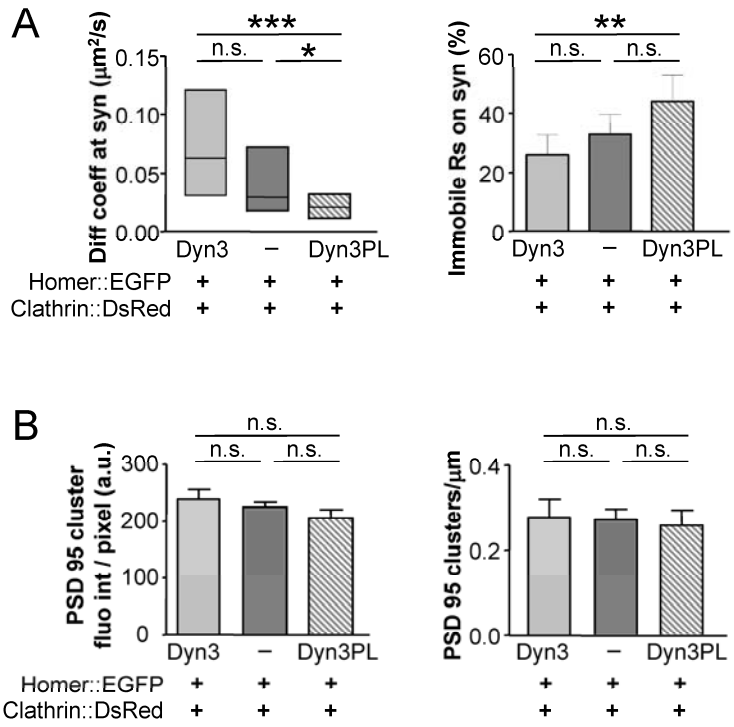
A
***
n.s.
*
Diff coeff at syn (µm²/s)
0.15
0.10
0.05
0.00
Dyn3
–
Dyn3PL
Homer::EGFP + + +
Clathrin::DsRed + + +
**
n.s.
n.s.
Immobile Rs on syn (%)
60
40
20
0
Dyn3
–
Dyn3PL
+ + +
+ + +
B
n.s.
n.s.
n.s.
PSD 95 cluster fluo int / pixel (a.u.)
300
200
100
0
Dyn3
–
Dyn3PL
Homer::EGFP + + +
Clathrin::DsRed + + +
n.s.
n.s.
n.s.
PSD 95 clusters/µm
0.4
0.2
0.0
Dyn3
–
Dyn3PL
+ + +
+ + +

Figure S7

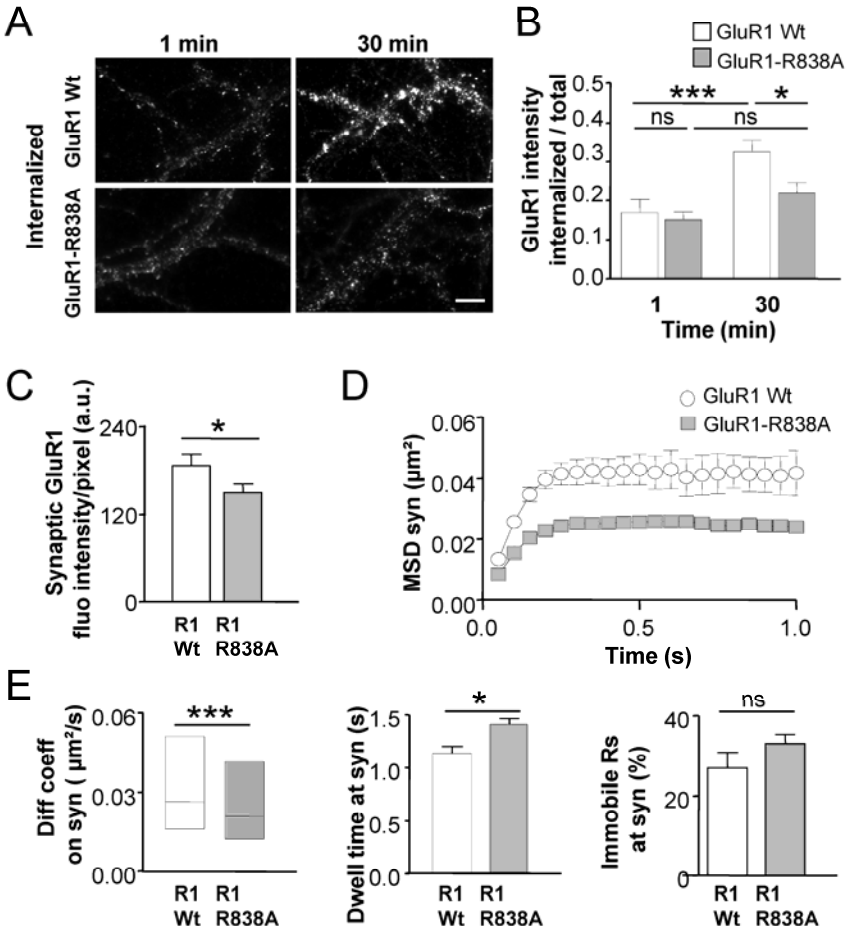
A
1 min
30 min
Internalized
GluR1 Wt
GluR1-R838A
B
GluR1 Wt
GluR1-R838A
GluR1 intensity internalized / total
***
*
ns
ns
Time (min)
C
Synaptic GluR1 fluo intensity/pixel (a.u.)
*
R1 Wt
R1 R838A
D
GluR1 Wt
GluR1-R838A
MSD syn (µm²)
Time (s)
E
Diff coeff on syn (µm²/s)
***
Dwell time at syn (s)
*
Immobile Rs at syn (%)
ns
R1 Wt
R1 R838A

Figure S8

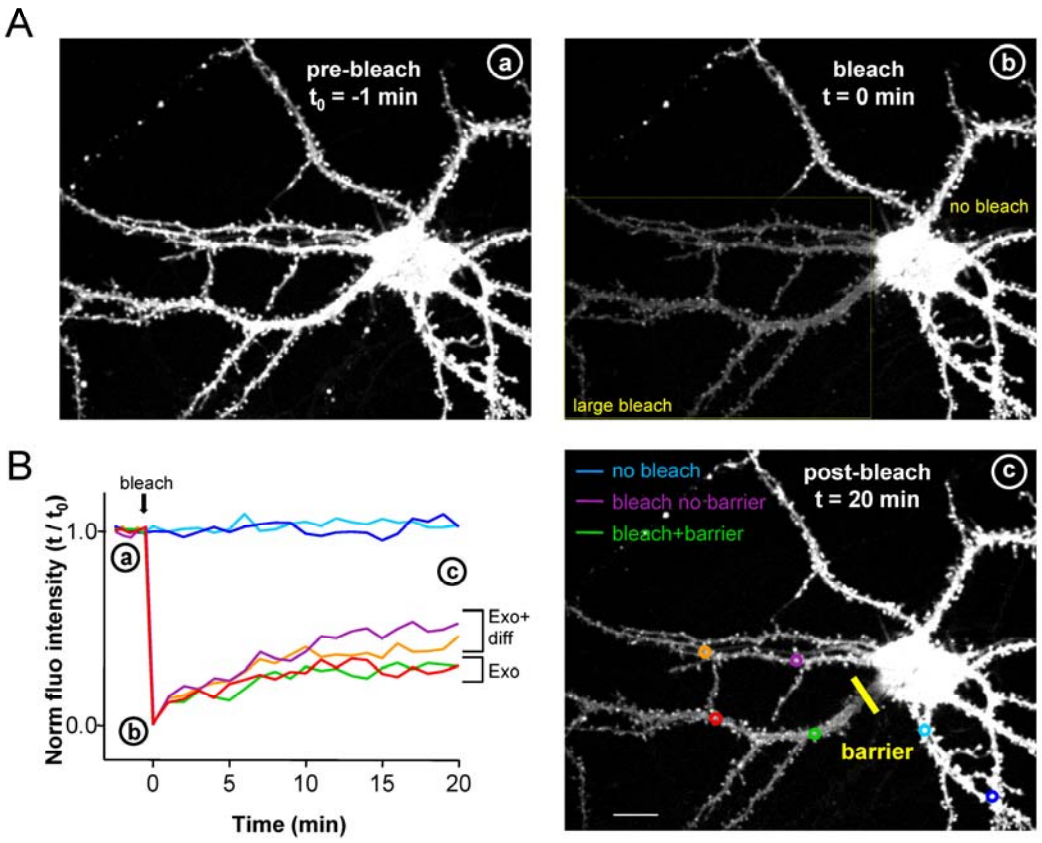
A
pre-bleach
t_0 = -1 min
a
bleach
t = 0 min
b
no bleach
large bleach
B
bleach
Norm fluo intensity (t / t_0)
1.0
0.0
a
b
c
Exo+
diff
Exo
0
5
10
15
20
Time (min)
no bleach
bleach no barrier
bleach+barrier
post-bleach
t = 20 min
c
barrier

Figure S9

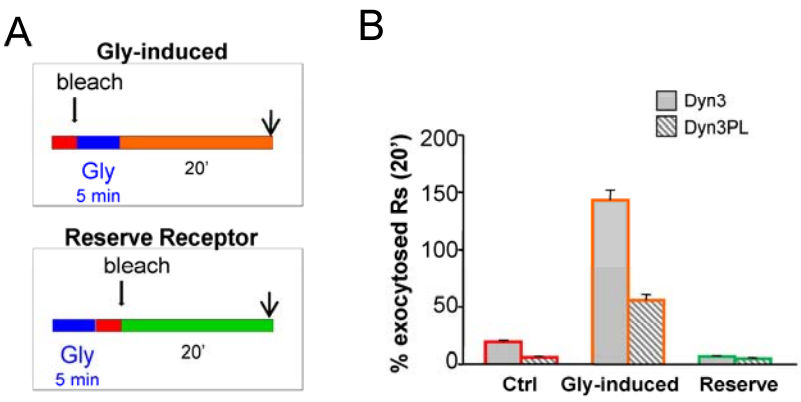
A
Gly-induced
bleach
Gly
5 min
20'
Reserve Receptor
bleach
Gly
5 min
20'
B
Dyn3
Dyn3PL
% exocytosed Rs (20')
200
150
100
50
0
Ctrl
Gly-induced
Reserve

Supplementary Fig. 10